Modelling the seismic resistance of retaining structures

Modèles de la résistance sismique des murs de soutènement

M. D. BOLTON, Cambridge University Engineering Department, Cambridge, UK
R. S. STEEDMAN, Cambridge University Engineering Department, Cambridge, UK

SYNOPSIS New data are presented of the behaviour of model walls retaining dry sand which were subjected to episodes of base shaking in the Cambridge Geotechnical Centrifuge. Instrumentation permits the back-analysis of failures, leading to an estimate of mobilised angles of shearing in the soil. Under certain circumstances, the sliding of rectangular mass walls was seen to provoke progressive strain-softening in localised shear zones. This contrasted to the ultimate behaviour of fixed-base cantilever wall stems which engendered more uniform soil strains when they rotated about a plastic hinge at their base. The consequences of progressive failure, both for research methodology and design practice, are explored.

INTRODUCTION

Notwithstanding the evidence of damage to earth retaining structures during earthquakes, there is a lack of well-instrumented back-analyses at full-scale. New analytical techniques have usually been justified in relation to the behaviour of small models subject to lateral shaking. Comparisons between the behaviour of mass walls and cantilever walls have been especially difficult since the similarity conditions for the deformation and failure of reinforced concrete cantilevers are very difficult to achieve at reduced stress levels. Indeed, the strength and stiffness of soils under very small confining pressures are very difficult to measure using standard equipment. Nor is there complete confidence, should these problems be resolved, that the enhanced rate of dilation in these conditions will lead to overall similarity in behaviour between a reduced-scale reduced-stress model and a full-scale prototype.

Centrifugal modelling, however, results in the duplication of all prototype stresses within a 1/n scale model accelerated to n gravities. Schofield (1981) outlines the development of the technique at Cambridge, including the additional criteria necessary for the achievement of dynamic similarity. In essence, imposed accelerations must be enhanced by the factor n in harmony with the reduced scale of the model boundaries. Taken together, this implies that the frequency of imposed oscillations must be increased by factor n.

Fixed-base cantilever walls

Initial studies of the behaviour of fixed-base microconcrete cantilever walls were reported by Bolton and Steedman (1982). A calculation based on the quasi-static wedge analysis of Okabe (1924) and Mononobe and Matsuo (1929), herein after referred to as the M-O analysis, was found to offer a reasonable estimate of the base acceleration required to promote yield of the reinforcement and plastic hinge rotation at the base of the stem.

Subsequent work has been undertaken using the Bumpy Road shaking facility described by Kutter (1982). Ten roughly sinusoidal cycles of 'horizontal' (tangential) base shaking can be imposed in any one event, but similar events can be successively reimposed with separately specified acceleration amplitudes up to 40% (e.g. at 80g the maximum amplitude of lateral shaking is 40% x 80g = 32g), without stopping the centrifuge. Bolton and Steedman (1984) report two further tests on fixed-base microconcrete models, together with a series of tests on Dural walls of similar characteristics. The dispositions of the models are typified in Fig.1.

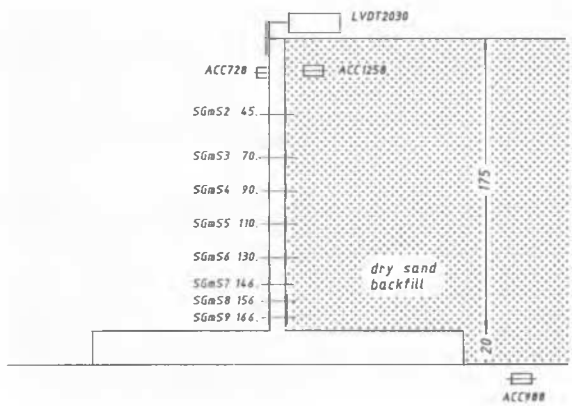

Fig.1 Typical Section of a Fixed-base Cantilever Model (dimensions in mm)

The dry Leighton-Buzzard 14/25 sand was known to have an ultimate angle of shearing in a critical state of Φ_{crit} between 33° and 35°, Stroud (1971). When maximally dense the same sand was found to mobilise $\Phi_{max} = 50°$ in plane strain at stress levels ($p' = 80$ kN/m²) consistent with the typical active states behind the model walls, before dilatant softening within shear bands reduced Φ to Φ_{crit}.

It was therefore encouraging to discover that prior to any shaking, the bending moments inferred from strain gauge bridges at various positions on the aluminium walls retaining very dense sand were consistent with $\Phi = 54°$, and wall friction $\delta = 20°$, used in conjunction with simple wedge theory and an assumed triangular active earth pressure distribution. Observed 'static' wall displacements were consistent with $\Phi = 50°$, $\delta = 20°$. Peak bending moments observed during shaking episodes were closely in agreement with the sum of wall inertia moment and M-O moment, again assuming a triangular earth pressure distribution, and again using $\Phi = 50°$, $\delta = 20°$. Typical errors were within 10% for small displacements of the aluminium walls.

In comparison with the statically measured yield moment of the two microconcrete walls the same technique, using $\Phi = 50°$ and $\delta = 30°$, underpredicted the base moment at observed yield accelerations during shaking by margins of 7% and 23%. This could imply that with plastic wall rotations of the order of 1.3° the mobilisable angle of soil shearing had reduced Φ to 47° and 43° respectively.

Mass Walls

A number of rectangular mass walls of stiff plywood construction have been subjected to episodes of base shaking using the Bumpy Road actuator. Fig.2 depicts a typical configuration, used in test RSS.81 at 80 gravities. This corresponded to a test of a prototype 10.8 m high and 7.2 m wide with an equivalent mass of 21,800 kg/m acting at a height of 3.6 m. The soil was dry and at a relative density of 92%, including the bed upon which the model rested which was 2.4 m deep at prototype scale. The model soil was 14/25 Leighton-Buzzard sand with a characteristic particle size of 0.9 mm : the particle size of an equivalent prototype is a topic for later discussion.

Sand particles were glued to the base of the model wall prior to placement to ensure a

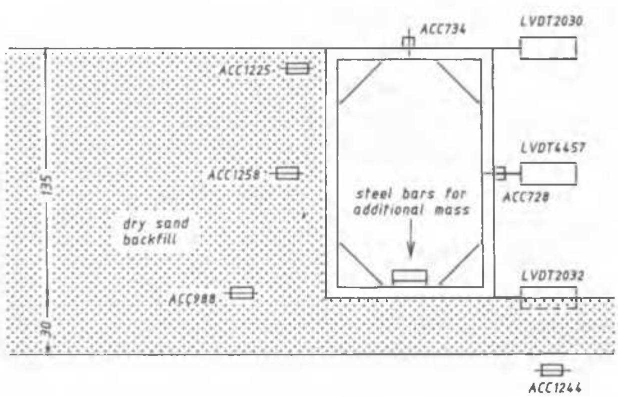

Fig.2 Section of Mass Wall Test RSS.81

rough surface contact. The retaining face of the wall was left smooth. Table I shows the mobilisation of shearing angle due to direct shear across the surface of samples mounted in a 60 mm square apparatus.

TABLE I

Mobilisation of shearing angle in direct shear

surface finish	relative density	displacement (mm) 2	4	6
smooth	70%	33°	33°	33°
glued sand	57%	44.6° peak	36°	34°

The response of model 81 to initial centrifuging was a rotation of 0.25° and a base translation of 0.07 mm. An initial earthquake of base input 21% caused a further 0.27° of rotation and a base slip of 0.32 mm. Fig.3 then shows the response to a second earthquake of base input 33 %. Fig.4 depicts the active wall failure at angle $\theta = 25.5°$ corresponding to the data in Fig.3. Small rotations over the first five pulses were followed during the second five by a continuous outward translation of 11 mm during which negligible rotations were monitored by the displacement transducers.

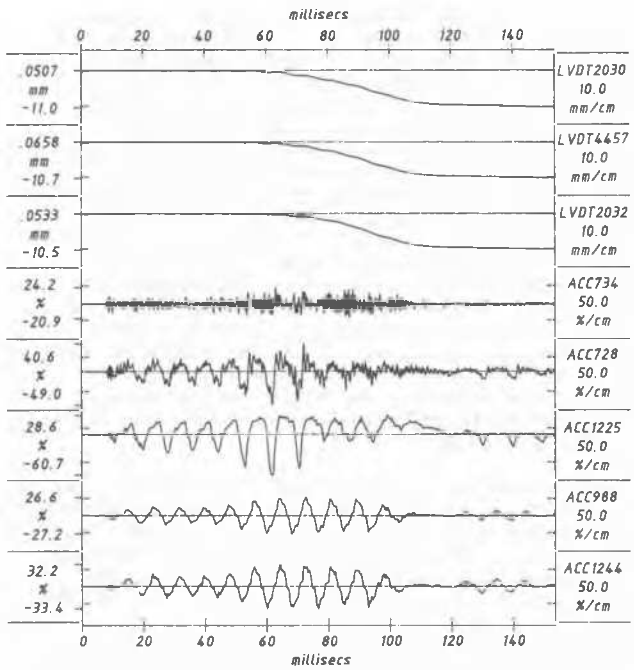

Fig.3 Test 81 Data Record (model units)

Double Block Idealisation

It was decided to model each instant during sliding failure using the double block idealisation of Zarrabi (1979), with acceleration components shown in Fig.5. The input acceleration component k_h was taken to be the response of the accelerometer placed in the sand at the level of the base of the wall. Experience proved that input $k_v = 0$, $k_h' = k_h''$ in the blocks horizontally, and $k_v'' = 0$ for the

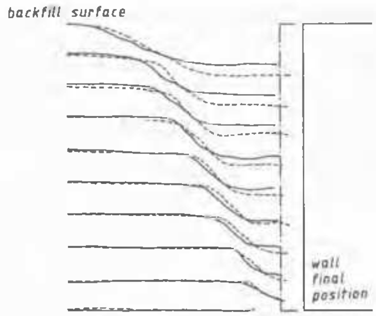

Fig.4 Test 81 Active Failure Wedge

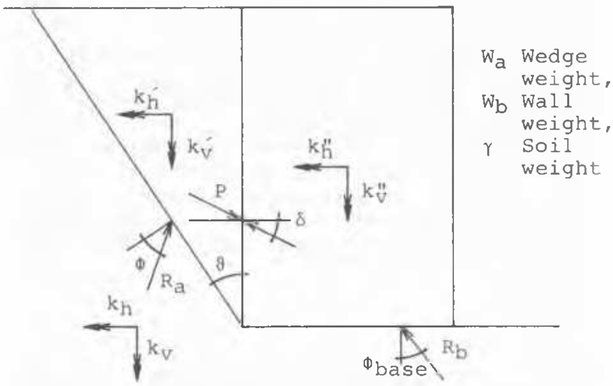

Fig. 5 Notation of Double Block Model

wall. Ignoring dilation, the triangle of fill was taken to have relative motion parallel to the slip plane. It follows that the induced vertical acceleration component in the triangle

$$k_v' = (k_h - k_h')/\tan\vartheta \qquad (1)$$

Reversing these accelerations to create D'Alembert body forces in Fig.5, and using

$$\tan\beta = k_h \quad \text{and} \quad \tan\beta' = k_h' \qquad (2)$$

it is easy to show that during sliding of the wall the inclined active thrust is given by

$$\frac{P}{W_b} = \frac{\tan\Phi_{base} - \tan\beta}{\cos\delta - \sin\delta\tan\Phi_{base}} \qquad (3)$$

The mobilised angle of shearing on the active plane can then be similarly determined to be

$$\tan\Phi = \frac{\cos\vartheta\left(1-\frac{\tan\beta}{\tan\vartheta}\right) + \frac{\tan\beta'}{\sin\vartheta} - \frac{P}{W_a}\sin(\vartheta+\delta)}{\frac{\sin(\vartheta-\beta)}{\cos\beta} + \frac{P}{W_a}\cos(\vartheta+\delta)} \qquad (4)$$

$$\text{where} \quad W_a = \frac{1}{2}\gamma H^2 \tan\vartheta \qquad (5)$$

In back-analysis the value of $\delta = 33°$ was known with great confidence. However, equations (3) and (4) can be used to authorise many combinations of Φ_{base} and Φ, any pair of which satisfy the kinematics. Fortunately the additional inequalities

$$33° < \Phi, \Phi_{base} < 50°$$

were often sufficient to determine values which appeared subjectively reasonable. Following the fixed-base wall analysis $\Phi = 50°$ was used as the starting strength of the fill behind every block wall which had not already slid more than about 2 mm. It then became obvious that Φ_{base} habitually took values around the critical state, circa 33° to 35°, at almost all stages of every earthquake on every model. Table II lists details of Φ_{base} and model characteristics used to predict Φ in Fig.7. Whatever the balance may have been between Φ and Φ_{base} in the earlier pulses it is clear that after 6 mm of sliding along the observed active failure plane, no soil element can develop more than 33° of friction, irrespective of its 92% relative density a few milliseconds before.

TABLE II

80g model failure details (ref. Fig.7)
All walls retained dry sand, units model scale.

Test code	wall height (mm)	wall width (mm)	wall mass (kg/m)	soil density (kg/m³)	Φbase initial (degrees)	final
62	90	135	2.06	1740	33	30.2
70	90	135	2.06	1770	33	33
71	135	90	3.61	1750	38	34
72	90	135	2.06	1610	34.5	33.5
81	90	135	3.41	1740	34.5	31
82	135	60	2.91	1740	30	30

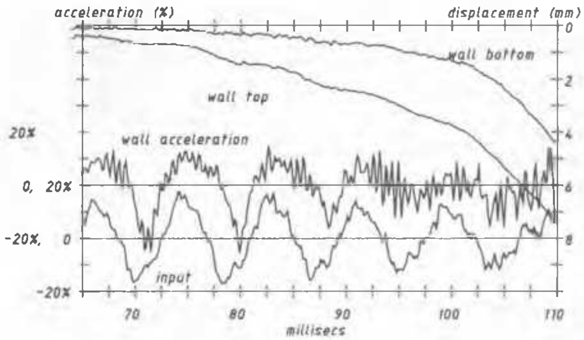

Fig.6 The Failure of Test 82

Similar events were recorded in a number of other models whose different properties are listed below those for test 81 in Table II. The consistency is encouraging. The occurrence of $\Phi_{base} = 30°$ even in the earlier stages of test 82 is, perhaps, worth explaining. This model was unusually narrow and therefore subject to large eccentricity and inclination of its base reaction. In addition, of course, it was resting on a soil bed which was suffering its own lateral body force. An approximate calculation based on the reduction factors of Meyerhof (1953) and (1957) showed that, using $\Phi_{base} = 30°$ and $\Phi = 45°$ in the soil bed, a bearing failure was imminent in a 15% earthquake. Movements were therefore triggered rather earlier than in other tests of wider walls. Fig.6 shows the development of displacements in test 82 during the last pulses of shaking. An accelerating displacement is seen coincident with the end of input shaking. At time 102 mS rotation is overtaken by a dramatic sliding instability as the soil on a slip plane softens to a critical state.

In considering why the soil at the base was so easily softened, three points might be made. Firstly, the wall may be free to dissipate dilatancy in the sand by engaging in vertical vibration. Secondly, once a little dilatancy had taken place at a few locations beneath the stiff wall, the whole base thrust will be transmitted through these softening locations : averaging for Φ will not take place between softened and unsoftened zones. Thirdly, the plane of sliding is absolutely determined, inviting the greatest possible degree of localisation of strains.

The data of Φ mobilised in the fill at particular sliding displacements $u = x/\sin\theta$ are collated in Fig.7. Included in the diagram are the results of test 72 using a finer, albeit more angular, grade of Leighton Buzzard sand (d_{50} = 0.225 mm). Although there is some scatter (2 to 5 mm) in the displacement required to initiate softening, there is a surprising uniformity in the further displacement (4 mm) required to complete the process. Expressed in terms of grain diameters, a slippage of the order of 10 d_{50} is required to drop Φ from 50° to 33°, thereby doubling the earth pressure coefficient.

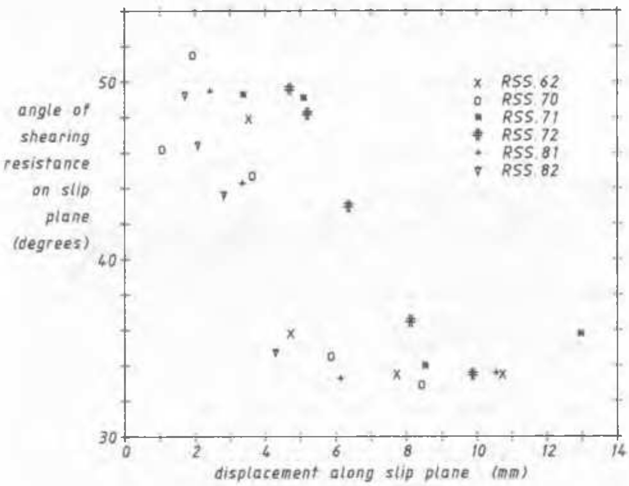

Fig.7 Φ vs. displacement on slip plane

CONCLUSIONS

1. Mass walls which were free to slide and rotate on a dense sand bed were shown to be highly susceptible to soil softening to Φ_{crit} = 33° on their foundation interface.

2. Fixed-base elastic cantilever walls had been seen to permit the mobilisation of a full plane strain angle of shearing, Φ = 50°, in the dense backfill reducing to about 45° after 1° of plastic hinge rotation in microconcrete models. The fill behind mass walls was seen, in contrast, to be much more vulnerable.

3. A tentative relationship was derived between Φ mobilised on the active slip plane and the magnitude of relative sliding along it. Slippages of between 6 and 9 mm were required before Φ dropped fully to Φ_{crit}. This might be expressed as roughly 10 particle diameters of sliding along a putative slip band 10 diameters in thickness, though the rate of softening of a 0.225 mm subangular sand was found to be similar to that of a 0.9 mm subrounded sand. In order to achieve similarity with the degree of softening in a full scale prototype, this might imply that particles should ideally be scaled down in size by the same factor n applicable to the model boundaries. Fine sand in the centrifuge might then model coarse gravel. On the other hand, 10 particle diameters is such a small relative slippage in a typical situation that it might alternatively be accepted that fully softened soil strengths Φ_{crit} be invariably used on slip surfaces in sand irrespective of soil density.

4. The prevention of sliding displacements in excess of about 10 particle diameters is necessary for dense soils if further violent movements consequent on strain softening are to be avoided. It may prove reasonable to use soil strengths somewhat greater than Φ_{crit} in circumstances of uniformly distributed soil strains at collapse (e.g. the plastic rotation of fixed-base cantilever stems). More model tests are called for.

REFERENCES

Bolton, M.D. & Steedman, R.S. (1982). Centrifugal testing of microconcrete retaining walls subjected to base shaking. Proc.Conf.Soil Dy. & E´quake Eng., Southampton, July, 311-329.

Bolton, M.D. & Steedman, R.S. (1984). The behaviour of fixed cantilever walls subject to lateral shaking. Pro.Conf.Appl´n.Cen´fuge Model´g to Geotec.Design, Manchester, April, 302-314.

Kutter, B.L. (1982). Centrifugal Modelling of the response of clay embankments to earthquakes. PhD Thesis, Cambridge University.

Meyerhof, G.G. (1953). The bearing capacity of foundations under eccentric and inclined loads Proc 3rd I.C.S.M.F.E., Zurich, VI, 440-445.

Meyerhof, G.G. (1957). The ultimate bearing capacity of foundations on slopes. Proc.4th I.C.S.M.F.E., London, VI, 384-386.

Mononobe, N. & Matsuo, M. (1929). On the determination of earth pressures during earthquakes. Proc.World Eng.Congress, 9.

Okabe, S. (1924). General theory of earth pressures. J.Japan Soc.Civil Eng., 12, 1.

Schofield, A.N. (1981). Dynamic and earthquake geotechnical centrifuge modelling. Proc.Int. Conf.Rec.Adv.Geotech.E´quake Eng. & Soil Dy., Missouri, April 26 - May 3.

Stroud, M.A. (1971). Sand at low stress levels in the S.S.A. PhD Thesis, Cambridge University

Zarrabi, K. (1979). Sliding of gravity retaining walls during earthquake considering vertical acceleration and changing inclination of failure surface. S.M. Thesis, M.I.T.